



A novel peptide shows excellent anti-HIV-1 potency as a gp41 fusion inhibitor

Wei Liu^{a,b}, Xiaohong An^{a,b}, Jiao Wang^b, Xiaoguang Zhang^b, Jianjun Tan^a, Zhixiang Zhou^{a,*}, Yi Zeng^{a,b,*}

^a College of Life Science and Bioengineering, Beijing University of Technology, Beijing 100124, China

^b State Key Laboratory for Infectious Disease Prevention and Control, National Institute for Viral Disease Control and Prevention, Chinese Centre for Disease Control and Prevention, Beijing 100052, China

ARTICLE INFO

Article history:

Received 20 December 2017

Revised 26 January 2018

Accepted 29 January 2018

Available online 31 January 2018

Keywords:

HIV-1

Peptide fusion inhibitor

Gp41

ELISA

Terminal half-life

ABSTRACT

Fusion inhibitors of HIV prevent the virus from entering into the target cell via the interaction with gp41, which stops the process of spatial rearrangement of the viral envelope protein. A series of peptides have been designed and screened to obtain a highly potent novel sequence. Among them, CT105 possesses the most potent anti-viral ability at low nanomolar IC₅₀ values against a panel of HIV-1 pseudoviruses from A, B, C and A₁/D subtypes, whereas T20 shows much weaker potency. CT105 also shows excellent inhibitory activity at 260 pico molar IC₅₀ against HIV-1 replication. As a fusion inhibitor, CT105 has a strong ability to interrupt gp41 core formation. The terminal half-life of CT105 possesses 1.72-fold longer than that of T20 as determined by developing an indirect competitive ELISA method. The results suggest that this artificial peptide CT105 could be a favorable archetype for further optimization and modification.

© 2018 Elsevier Ltd. All rights reserved.

The entry of human immunodeficiency virus (HIV) is triggered by recognition between envelope protein (env) on the virions and the CD4 receptor on the cell surface.^{1–3} Env is a trimeric glycoprotein composed of three copies of gp120/gp41 heterodimers that originate from precursor protein gp160.^{1,4} The inner domain of gp120 interacts with gp41, and its spatial rearrangement results in the dissociation of the gp120–gp41 complex and conformational changes of the gp41 domains in preparation for catalyzing membrane fusion.^{5,6} HIV fusion inhibitors are designed to prevent the virus from entering into host cells by blocking the gp41 conformational transition.⁷

Understanding the structure of gp41 at each step during HIV fusion is of fundamental significance in designing fusion inhibitors for preventing further infection. Gp41 is a 345-residue polypeptide from 512 to 856 of env according to the HXB2 HIV-1 strain.^{8,9} The N-terminal helical heptad repeat region (NHR) and the C-terminal helical heptad repeat region (CHR) form the six helix bundle (6-HB) that represents the gp41 core.¹

T20 (generic name: Enfuvirtide, brand name: Fuzeon) is a representative peptide fusion inhibitor and the only one that has been put into clinical use.¹⁰ However, its high-dosage injection requirements and rapid plasma clearance rate render it limit in salvage

treatment for cocktail resistant patients.⁸ Moreover, extended exposure, especially if the virus is not completely restrained, can cause viral resistance to T20.^{11,12} T20 could induce a mutant virus with high resistance (81-fold) to T20 in about one month.¹³

Because T20 can induce drug resistance, it is necessary to generate new peptide fusion inhibitors.¹⁴ Our group has previously designed a series of peptides based on the sequence of the CHR of gp41.¹⁵ Briefly, using CP621–652 as a peptide designing template, a series of systematic replacements were introduced to enhance the α -helicity of synthesized peptides that correlates with the anti-HIV activity. Charged residues were incorporated at favorable potentials for intra-helical salt-bridges, and alanine was introduced to promote helix formation. Initial screening showed CT105 as the most potent fusion inhibitor.

Molecular docking research has found that CT105 could wrap antiparallel to the trimetric N-terminal heptad repeat (NHR) of gp41 in a left-handed direction.¹⁵ It was suggested that six residues of CT105 (Met626, Thr627, Trp628, Trp631, Glu634 and Tyr638) might insert into the hydrophobic pocket of NHR.¹⁵ The core structure of gp41 and the binding pattern between CT105 and gp41 are presented in Fig. 1. The results of clear native polyacrylamide gel electrophoresis (CN-PAGE) showed the strong binding affinity of CT105 towards N36, a peptide that represents gp41 NHR. Interestingly, the binding mode seems rather complicated. As showed in Fig. 2(A), N36 could not migrate into the gel in CN-PAGE condition because of its positive charge properties. More than four

* Corresponding authors at: College of Life Science and Bioengineering, Beijing University of Technology, Beijing 100124, China (Y. Zeng).

E-mail addresses: zhouzhixiang@bjut.edu.cn (Z. Zhou), zengyi@public.bta.net.cn (Y. Zeng).

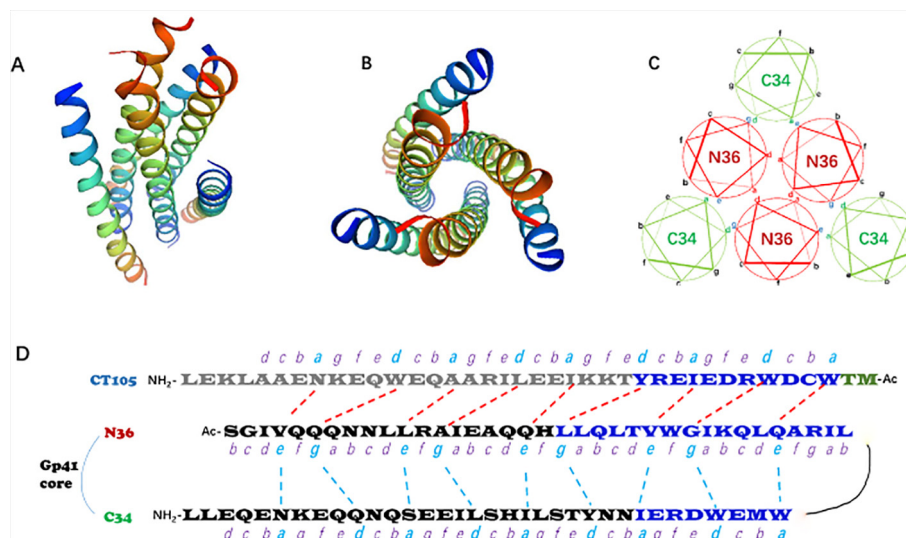


Fig. 1. The core structure of gp41 and CT105. (A) Lateral, (B) axial and (C) helical wheel representations of the 6-HB of gp41 (PDB 1AIK) formed by the N36 and C34 peptides. (C) Heptad-repeat positions are labeled (a) through (g). Residues at the (a), and (d) (shown in red) positions of three NHR interact with each other and constitute the central trimeric coiled-coil. The (a) and (d) residues in the CHR (shown in green) interact with the (e) and (g) sites on the central NHR coiled-coil (shown in blue), which constitutes a hydrophobic core of the trimer-of-hairpins. (D) Sequence of N36, C34 and CT105 and their binding sites.

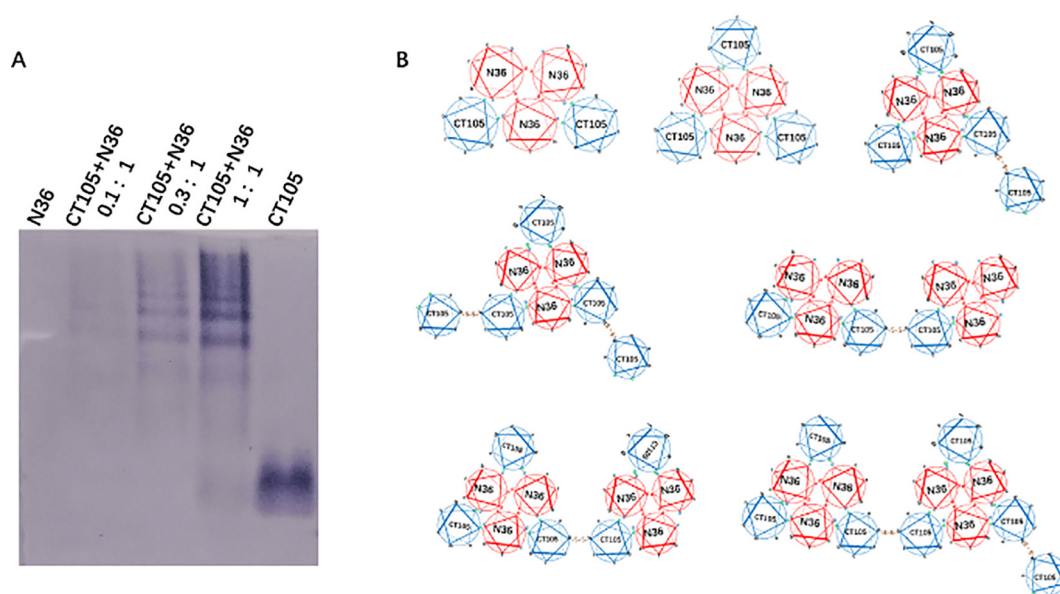


Fig. 2. (A) The CN-PAGE analysis of the interaction between HIV-1 gp41 N36 and CT105. Peptides were incubated at 37 °C for 30 min and then loaded into the polyacrylamide gel (12% separating gel, 4% stacking gel). Electrophoresis was carried out with 120 V constant voltage for 2 h. (B) Possible binding modes formed by N36, CT105 and CT105 dimers.

complexes could be found after incubation. When the N36 peptide was incubated with CT105, several bands appeared that represent the N36-CT105 complex. This indicates that not only 6-HB but also other unknown polymers are presented (see in Fig. 2). We speculate that CT105 might work as a dimer on account of the self-connection of its cysteine. During the incubation process, the CT105 moieties might suffer from slight oxidation that could cause the formation of the disulfide bond. That might be the main reason why so many different complexes are formed. We also observed the interaction among N36, CT105 and C34, a peptide that could form the 6-HB core of gp41 with N36. As presented in Fig. 3, N36 was mixed with C34 peptide at a 1:1 ratio. CT105, at different final concentrations of 5 μ M, 15 μ M, 25 μ M and 50 μ M, was incubated with the mixture of C34 and N36. Results showed that CT105

rather than C34 had strong affinity towards N36. CT105 could bind with N36 in a dose-independent manner. The CT105-N36 complex formed when the concentration of CT105 was 10-fold less than that of C34. In addition, C34 exhibited little effect on CT105-N36 disassociation, even if the C34 peptide concentration was high.

To test the inhibitory potency of CT105 against HIV-1, TZM-bl cells were infected with a panel of different subtypes of HIV-1 pseudoviruses. The TZM-bl cells were derived from Hela cells, which express CD4 and CXCR4 as well as CCR5 receptor, and contain the firefly luciferase, LacZ reporter under the control of a Tat-responsive reporter for quantification.¹⁶ The peptides were prepared with six series of dilutions in a 4-fold stepwise manner, and added to TZM-bl cells together with 100TCID₅₀ of each subtype of HIV-1 pseudoviruses. After 48 h incubation at 37 °C, the

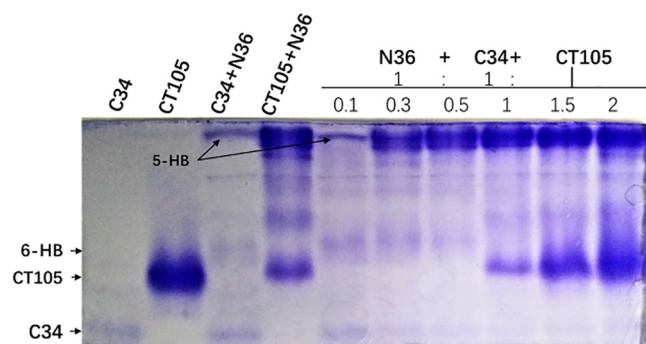


Fig. 3. The CN-PAGE analysis of the interaction among HIV-1 gp41 N36, C34 and CT105. Peptides were incubated at 37 °C for 30 min. Electrophoresis was carried out with 120 V constant voltage for 1 h.

luciferase expressed by Tzm-bl cells were determined via luciferase assay reagents.

Peptide CT105 exhibited its potent activity to stop the entry of diverse HIV-1 variants in a single-cycle infection assay, whereas the inhibition ability of the approved peptide T20 was much weaker. One of the difficulties to block HIV-1 is the extremely high genetic variability of the virus, which results in many circulating recombinant forms. T20 is a peptide derived from the HIV-1 HXB2 strain *per se*. Therefore, it is easy to understand why T20 does not work well on many variants. In sharp contrast with T20, CT105 exhibits a certain degree of effect with the IC₅₀ values of 1.01–26.04 nM to inhibit HIV-1 pseudoviruses derived from A, B, C and A₁/D subtypes as showed in Table 1. In contrast, T20 had no inhibitory activity at concentration of 500 nM on some variants. These results indicate that CT105 has potent and broad anti-HIV activity.

Having defined the activity of CT105 against pseudoviruses, we further determined its activity in terms of anti-HIV-1 replication. Inhibition of the peptides on HIV-1 R3A and JRCSF was performed in the same procedure as for pseudoviruses. As shown in Fig. 4 and Table 2, CT105 possesses outstanding activity against HIV-1 with IC₅₀ under nanomolar levels against HIV-1 R3A and at low nanomolar concentration against HIV-1 JRCSF.

In order to define the pharmacokinetic profiles of CT105 for the investigation of whether CT105 has a longer terminal half-life than that of T20, we prepared the rabbit polyclonal antibodies of CT105 and utilized the indirect competitive enzyme linked immunosorbent assay (IC-ELISA) method for quantification. It was considered to be an efficient method for the quantification of small molecules as well as peptides.^{17–20} CT105 possesses no immunogenicity, hence we conjugated the peptide to keyhole limpet hemocyanin (KLH) and bovine serum albumin (BSA) separately by 1-ethyl-3-

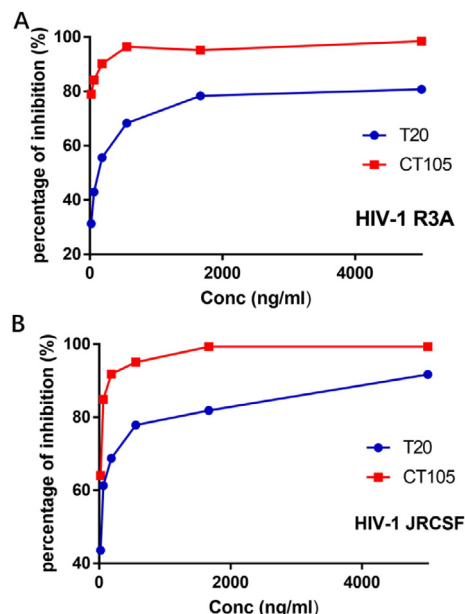


Fig. 4. (A) Inhibitory activities against HIV-1 JRCSF replication. (B) Inhibitory activities against HIV-1 R3A replication.

(3-dimethylaminopropyl) carbodiimide hydrochloride (EDAC) to make immunogen and coating antigen. New Zealand white rabbit was given the hypodermic injections of KLH coupled CT105 conjugate. First, 800 µg total protein administration mixed with Complete Freund's Adjuvant in a 1:1 ratio. Then, the rabbit was boosted three times with KLH-CT105 (400 µg) mixed with incomplete Freund's Adjuvant (1:1) at a 3-week interval. The anti-serum was collected and filtered. After that, the polyclonal antibodies of CT105 (pAb-CT105) were purified by antigen-immunoaffinity chromatography from the anti-serum.

After the preparation of pAb-CT105, IC-ELISA was well established. A 96-well polystyrene microplate was coated with BSA-CT105 conjugate in carbonate buffer, pH 9.6 at 4 °C overnight. The remaining active sites on the plate were blocked by the addition of blocking buffer (5% skimmed milk). The serially diluted CT105 peptide, utilized as standard solution to make the standard curve, negative control, and diluted unknown samples was incubated with pAb-CT105. 30 min after incubation at 37 °C the plate was washed and the diluted Peroxidase Horseradish (HRP) coupled anti-rabbit IgG then was added to wells and incubated at 37 °C for 30 min. After the plate was washed completely, a solution of 3,3',5,5'-tetramethylbenzidine (TMB) reagent was added and incubated, resulting in the development of a blue color. The color

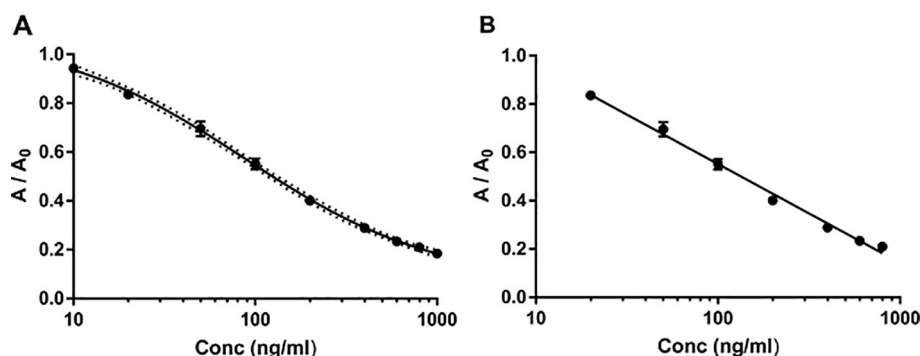
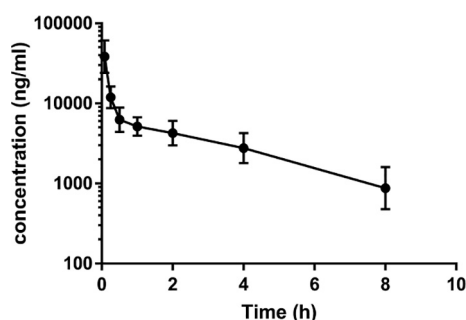
Table 1
Activity of T20 and CT105 for HIV-1 single-cycle infection Env clone Subtype T20 CT105.

Env clone	Subtype	T20		CT105	
		IC ₅₀ (nM)	95% CI	IC ₅₀ (nM)	95% CI
Q259env.w6	A	>500	–	15.77	14.27–35.22
Q842env.d16	A	>500	–	26.04	19.26–35.19
SC 422661.8	B	20.77	0.23–78.61	2.88	2.69–3.07
TRO.11	B	264.81	261.9–738.1	2.22	2.11–2.33
Du422.1	C	67.73	49.82–89.71	3.29	2.94–3.67
ZM197M.PB7	C	64.03	41.73–529.62	6.13	5.46–6.75
ZM53M.PB12					
ZM109F.PB4					
ZM53M.PB12	C	431.4	–	11.85	10.33–13.61
ZM109F.PB4					
ZM109F.PB4	C	>500	–	10.69	7.79–14.40
QA790.204I.ENV.C1	A ₁ /D	>500	–	1.02	0.79–1.26

Table 2

Activity of T20 and CT105 against HIV-1 replication Env clone Subtype T20 CT105.

HIV-1 variant	Subtype	T20		CT105	
		IC ₅₀ (nM)	95% CI (nM)	IC ₅₀ (nM)	95% CI (nM)
R3A	B	19.25	8.94–34.45	0.26	0.04–0.73
JRCSF	B	6.63	3.61–10.28	2.17	1.42–2.88

**Fig. 5.** (A) Standard curve of indirect competitive ELISA. (B) Linear range of the standard curve. A represents the OD value of samples; A₀ represents the blank OD value.**Fig. 6.** Plasma concentration of CT105 in rats.

development was stopped by the addition of stop solution (2 M H₂SO₄). The limit of detection was 7.9 ng/ml, limit of quantification was 20 ng/ml, and the linear range was 20–800 ng/ml. The standard curve is shown in Fig. 5.

To determine the terminal half-life of CT105, four Sprague Dawley rats were administered a single dose of CT105 (6 mg/kg in phosphate buffer) intravenously via the tail vein. Animals were treated in accordance with the Animal Welfare Act and the “Guide for the Care and Use of Laboratory Animals” (NIH Publication 86-23, revised 1985). Serial blood samples were collected from each animal before injection and at 0.08, 0.25, 0.5, 1, 2, 4 and 8 h after injection in tubes containing EDTA. The plasma samples were acquired after centrifuging (2500 rpm for 10 min at 4 °C). The plasma samples were examined and the concentrations of each sample were given by the interplot of GraphPad Prism software from the standard curve. The observed T_{1/2} of CT105 was 2.7 h, 1.72-fold longer than the 1.57 h half-life reported for T20.²¹ The concentrations of CT105 were sharply decreased within 30 min, followed by a comparatively slow elimination. The artificial peptide may be relatively insensitive to the proteolytic enzymes compared to T20, which caused the prolonged half-life of CT105 (Fig. 6).

In conclusion, CT105 could be an outstanding lead archetype for peptide drug design on account of its excellent activity against HIV. We believe that CT105 is expected to have much higher genetic barrier to resistance than T20 because CT105 contains pocket

binding domain (PBD), while T20 lacks PBD. Dwyer et al.¹³ carried out a passaging experiment and showed a PBD-containing CHR-peptide failed to induce a resistant strain in more than two months in culture. Further modification of CT105 peptide might be necessary for the improvement of pharmacokinetics profiles and the elongation of the terminal half-life. Several conjugation methods could make up this shortage.^{7,22–29} For example, the half-life of T20 was enhanced over 10-fold by PEG modification and over 20-fold by XTEN conjugation.³⁰ The pharmacokinetic profiles of peptide fusion inhibitors could also be promoted by antibodies, which also show the enhanced potency by their target-specific function.³¹ In the future, we will introduce these modifications to CT105 for better protein therapeutics.

Acknowledgement

We thank the National Natural Science Foundation of China (Grant No. 21677006) for financial support.

References

- Markosyan RM, Cohen FS, Melikyan GB. *Mol Biol Cell*. 2003;14:926–938.
- Bianchi E, Finotto M, Ingallinella P, et al. *Proc Natl Acad Sci USA*. 2005;102:12903–12908.
- Dimitrov AS, Louis JM, Bewley CA, Clore GM, Blumenthal R. *Biochemistry*. 2005;44:12471–12479.
- Chan DC, Fass D, Berger JM, Kim PS. *Cell*. 1997;89:263–273.
- Eckert DM, Kim PS. *Proc Natl Acad Sci USA*. 2001;98:11187–11192.
- Haqqani AA, Tilton JC. *Antiviral Res*. 2013;98:158–170.
- Liu W, Tan J, Mehryar MM, Teng Z, Zeng Y. *Med Chem Commun*. 2014;5:1472–1482.
- Naider F, Anglister J. *Curr Opin Struct Biol*. 2009;19:473–482.
- Huang JH, Lu L, Lu H, Chen X, Jiang S, Chen YH. *J Biol Chem*. 2007;282:6143–6152.
- Yao X, Chong H, Zhang C, et al. *J Biol Chem*. 2012;287:6788–6796.
- Tan JJ, Ma XT, Liu C, Zhang XY, Wang CX. *Curr Pharm Des*. 2013;19:1810–1817.
- Chong H, Yao X, Qiu Z, et al. *FASEB J*. 2013;27:1203–1213.
- Dwyer JJ, Wilson KL, Davison DK, et al. *Proc Natl Acad Sci USA*. 2007;104:12772–12777.
- Yu F, Lu L, Du L, Zhu X, Debnath AK, Jiang S. *Viruses*. 2013;5:127–149.
- Tan J, Su M, Zeng Y, Wang C. *Bioorg Med Chem*. 2016;24:201–206.
- Wang S, Sun W, Hu Q, Yan H, Zeng Y. *Bioorg Med Chem Lett*. 2017;27:2357–2359.
- Kumar A, Pulicherla KK, Sambasiva Rao KR. *J Immunoassay Immunochem*. 2016;37:228–242.
- Saeed A, Ling S, Yuan J, Wang S. *Toxins (Basel)*. 2017;9:8.
- Kohl TO, Ascoli CA. *Cold Spring Harb Protoc*. 2017;2017, pdb prot093757.

20. He S, Li X, Gao J, Tong P, Chen H. *Food Chem.* 2017;227:33–40.
21. Zhu X, Zhu Y, Ye S, et al. *Sci Rep.* 2015;5:13028.
22. Xie D, Yao C, Wang L, et al. *Antimicrob Agents Chemother.* 2010;54:191–196.
23. Stoddart CA, Nault G, Galkina SA, et al. *J Biol Chem.* 2008;283:34045–34052.
24. Wang C, Shi W, Cai L, et al. *J Med Chem.* 2013;56:2527–2539.
25. Ingallinella P, Bianchi E, Ladwa NA, et al. *Proc Natl Acad Sci USA.* 2009;106:5801–5806.
26. Hollmann A, Matos PM, Augusto MT, Castanho MA, Santos NC. *PLoS One.* 2013;8:e60302.
27. Lim SI, Mizuta Y, Takasu A, Hahn YS, Kim YH, Kwon I. *J Control Release.* 2013;170:219–225.
28. Lev N, Shai Y. *J Mol Biol.* 2007;374:220–230.
29. Khandare J, Minko T. *Prog Polym Sci.* 2006;31:359–397.
30. Ding S, Song M, Sim BC, et al. *Bioconjug Chem.* 2014;25:1351–1359.
31. Chang CH, Hinkula J, Loo M, et al. *PLoS One.* 2012;7:e41235.